Patterns of Lymphadenopathy in Thoracic Malignancies[1]

Amita Sharma, FRCR, Panos Fidias, MD, L. Anne Hayman, MD, Susanne L. Loomis, MS, Katherine H. Taber, PhD and Suzanne L. Aquino, MD

[1] From the Departments of Radiology (A.S., S.L.L., S.L.A.) and Medicine (P.F.), Massachusetts General Hospital, Harvard Medical School, 55 Fruit St, Founders 202, Boston, MA 02114; and the Department of Radiology and Herbert J. Frensley Center for Imaging Research, Baylor College of Medicine, Houston, Tex (L.A.H., K.H.T.). Presented as an education exhibit at the 2002 RSNA scientific assembly. Received March 19, 2003; revision requested April 29; final revision received November 6; accepted November 7. **Address correspondence to** A.S. (e-mail: *asharma2@partners.org*).

Abstract

There are different lymphatic drainage pathways in the thorax that are relevant in the staging of lung cancer, breast cancer, lymphoma, esophageal cancer, and malignant mesothelioma. To properly search for metastatic spread, it is important to carefully evaluate the specific nodal stations that drain the thoracic structures from which a primary tumor originates. Because size criteria have limitations in the prediction of nodal status, pathologic confirmation is essential for accurate staging. Computed tomography (CT) is useful in helping the surgeon or interventional radiologist determine the most appropriate approach for nodal sampling. Fluorine-18 fluorodeoxyglucose (FDG) positron emission tomography (PET) has an increasing role in detection of diseased lymph nodes that appear normal at CT alone, particularly when FDG PET images are fused with CT images. However, the role of radiologic imaging extends beyond initial staging and the guidance of interventions to include posttreatment assessment and the detection of recurrent disease. Therefore, at all levels of cancer imaging, it is essential to identify the relevant lymph node regions and their relations to the primary tumor.

Index Terms: Breast neoplasms, metastases, 00.32 • Esophagus, neoplasms, 71.32 • Lung neoplasms, metastases, 60.32 • Lymphatic system, CT, 99.1291 • Lymphatic system, neoplasms, 99.83 • Lymphoma, staging, 99.834 • Mesothelioma, 66.3254 • Thorax, neoplasms, 99.83

Introduction

The accurate classification of nodal involvement in a patient with malignancy is important. Computed tomography (CT) is the primary modality for imaging malignancy in the chest. It is used in staging the disease, planning treatment, evaluating response, and estimating prognosis. Knowledge of the drainage pathways of different malignancies is extremely useful as it directs the radiologist to the relevant nodal stations. Radiologists should therefore be aware of the criteria for evaluating mediastinal lymphadenopathy, the sites of the thoracic lymph nodes, and the limitations of CT.

Nodal tissue is present within the mediastinum and is often seen at chest CT. It is mainly situated around the distal trachea, carina, and main bronchi (1).

Autopsy studies and CT studies confirm that the average sizes of normal **lymph nodes** vary depending on their region (2–4). The majority of CT studies record the short-axis diameter of a **lymph** node, as this is the most reproducible measurement (3). Low paratracheal and subcarinal **nodes** can measure up to 11 mm in short-axis diameter. **Nodes** in the superior mediastinum and high paratracheal space are generally smaller and measure up to 7 mm. Normal right hilar and periesophageal **nodes** can be up to 10 mm in diameter, and left hilar and periesophageal **nodes** can be up to 7 mm in short-axis diameter. To simplify measurements, a **lymph** node in the paratracheal, hilar, subcarinal, paraesophageal, paraaortic, or subaortic region is generally considered enlarged if the short-axis diameter is greater than or equal to 10 mm (3,5).

There are very few data on the size of thoracic **lymph nodes** outside the mediastinum. Peridiaphragmatic **nodes** are considered abnormal if greater than 5 mm in short-axis diameter (6). No size criteria are available for internal mammary, retrocrural, and extrapleural **nodes**, and detection of these **nodes** should be considered abnormal.

There are limitations to use of size criteria to determine the presence or absence of nodal metastases, since metastases occur in normal-sized **nodes** and nodal enlargement can be secondary to benign conditions such as granulomatous disease (7).

Evaluation of the mediastinum for the presence of metastatic nodal disease with fluorine-18 fluorodeoxyglucose (FDG) positron emission tomography (PET) involves assessment of metabolic activity rather than node size. FDG PET has been shown to reflect metastatic involvement more accurately than CT (8,9). The poor anatomic resolution of FDG PET may be overcome with CT and FDG PET fusion imaging, whereby the site of increased uptake at FDG PET can be accurately defined with CT.

The International **Lymph** Node Classification and the International System for Staging Lung Cancer adopted by the American Joint Committee on Cancer (AJCC) and the Union Internationale Contre le Cancer (UICC) have defined the **lymph** node stations in the hila and mediastinum that are relevant to the staging of lung cancer (10). These stations can be applied to tumors of the breast, esophagus, and pleura and to **lymph**omas. However, additional **lymph** node regions in the thorax that are not included in this nomenclature can also be involved by tumor metastases.

This article describes the normal drainage pathways of the lung, breast, esophagus, and pleura. The sites of nodal metastases and their relevance in staging are presented with clinical radiologic examples. The role and limitations of imaging techniques, especially CT, are evaluated.

Lung Cancer

The lungs have a rich **lymph**atic supply that consists of a pleural and parenchymal network (11). The pleural **lymph**atics course over the parietal and visceral pleural surfaces and drain into the medial aspect of the lung near the hilum, where they anastomose with the parenchymal **lymph**atics. The parenchymal **lymph**atics are located in the interlobular septa and bronchovascular bundles. Multiple **lymph**atic channels anastomose with each other before draining sequentially into the intralobular, interlobular, lobar, and finally the hilar **nodes**. The entire **lymph**atic system clears interstitial fluid from the lungs and removes foreign particles and antigens. This pathway is also responsible for the spread of tumor from the lung to the hilum and subsequently into the mediastinum.

The hilar **nodes** drain into the mediastinum, but the **mediastinal** pathways are variable and are related to the lobe of origin of the pulmonary **lymph**atics. Studies of lung cancer in various lobes confirm that nodal pathways are largely dependent on the lobar origin of the tumor (Fig 1) (12,13). Most parenchymal tumors drain to the hilar **nodes** before reaching the

mediastinum. Lesions of the right upper lobe predominantly then drain into the right paratracheal and anterior **mediastinal nodes**. Right middle and lower lobe tumors predominantly drain into the subcarinal **nodes** and subsequently into the right paratracheal and anterior **mediastinal nodes**. Left upper lobe tumors drain to the subaortic and paraaortic **nodes**, and left lower lobe tumors drain to the subcarinal and subaortic **nodes**.

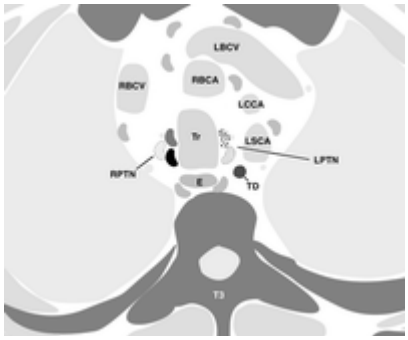

View larger version (28K):
[in this window]
[in a new window]
[Download PPT slide]

Figure 1a. Diagrams of the axial anatomy of the chest show the **lymph nodes** and drainage pathways for lung cancer in different lobes of the lung. All tumors drain to the interlobar and hilar **nodes**. The separate drainage pathways for tumors of the right upper lobe (black **nodes**), middle lobe (dark gray **nodes**), right lower lobe (striped **nodes**), left upper lobe (crosshatched **nodes**), and left lower lobe (dotted **nodes**) are shown. The corresponding American Thoracic Society (ATS) stations are labeled. ***E*** = esophagus, ***TD*** = thoracic duct. **(a)** Diagram shows the left paratracheal **nodes** *(LPTN)* (ATS station 2L) and right paratracheal **nodes** *(RPTN)* (ATS station 2R). *LBCV* = left brachiocephalic vein, *LCCA* = left common carotid artery, *LSCA* = left subclavian artery, *RBCA* = right brachiocephalic artery, *RBCV* = right brachiocephalic vein, *Tr* = trachea. **(b)** Diagram shows the left paratracheal **nodes** *(LPTN)* (ATS station 4L), right paratracheal **nodes** *(RPTN)* (ATS station 4R), and subaortic **nodes** *(SAN)* (ATS station 5). *AA* = ascending aorta, *Ao* = aorta, *SVC* = superior vena cava, *Tr* = trachea. **(c)** Diagram shows the hilar **nodes** *(HN)* (ATS station 10), interlobar **nodes** *(ILN)* (ATS station 11), lobar **nodes** *(LN)* (ATS station 12), and subcarinal **nodes** *(SCN)* (ATS station 7). *Ao* = aorta, *BI* = bronchus intermedius, *LMB* = left main bronchus, *LPA* = left pulmonary artery, *LULB* = left upper lobe bronchus, *PA* = pulmonary artery, *RPA* = right pulmonary artery, *SPV* = superior pulmonary vein, *SVC* = superior vena cava. **(d)** Diagram shows the left inferior pulmonary ligament node *(LIPLN)* (ATS station 9) and right inferior pulmonary ligament node *(RIPLN)* (ATS station 9). *Ao* = aorta, *CS* = coronary sinus, *ECF* = epicardial fat, *LV* = left ventricle, *RA* = right atrium, *RV* = right ventricle.

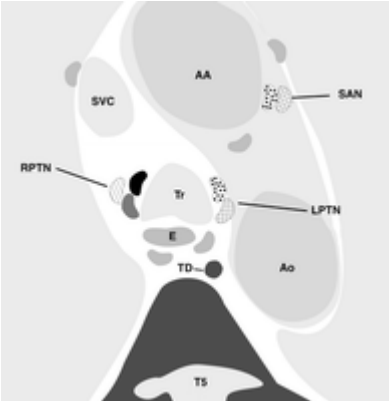

View larger version (25K):
[in this window]
[in a new window]
[Download PPT slide]

Figure 1b. Diagrams of the axial anatomy of the chest show the **lymph nodes** and drainage pathways for lung cancer in different lobes of the lung. All tumors drain to the interlobar and hilar **nodes**. The separate drainage pathways for tumors of the right upper lobe (black **nodes**), middle lobe (dark gray **nodes**), right lower lobe (striped **nodes**), left upper lobe (crosshatched **nodes**), and left lower lobe (dotted **nodes**) are shown. The corresponding American Thoracic Society (ATS) stations are labeled. ***E*** = esophagus, ***TD*** = thoracic duct. **(a)** Diagram shows the left paratracheal **nodes** *(LPTN)* (ATS station 2L) and right paratracheal **nodes** *(RPTN)* (ATS station 2R). *LBCV* = left brachiocephalic vein, *LCCA* = left common carotid artery, *LSCA* = left subclavian artery, *RBCA* = right brachiocephalic artery, *RBCV* = right brachiocephalic vein, *Tr* = trachea. **(b)** Diagram shows the left paratracheal **nodes** *(LPTN)* (ATS station 4L), right paratracheal **nodes** *(RPTN)* (ATS station 4R), and subaortic **nodes** *(SAN)* (ATS station 5). *AA* = ascending aorta, *Ao* = aorta, *SVC* = superior vena cava, *Tr* = trachea. **(c)** Diagram shows the hilar **nodes** *(HN)* (ATS station 10), interlobar **nodes** *(ILN)* (ATS station 11), lobar **nodes** *(LN)* (ATS station 12), and subcarinal **nodes** *(SCN)* (ATS station 7). *Ao* = aorta, *BI* = bronchus intermedius, *LMB* = left main bronchus, *LPA* = left pulmonary artery, *LULB* = left upper lobe bronchus, *PA* = pulmonary artery, *RPA* = right pulmonary artery, *SPV* = superior pulmonary vein, *SVC* = superior vena cava. **(d)** Diagram shows the left inferior pulmonary ligament node *(LIPLN)* (ATS station 9) and right inferior pulmonary ligament node *(RIPLN)* (ATS station 9). *Ao* = aorta, *CS* = coronary sinus, *ECF* = epicardial fat, *LV* = left ventricle, *RA* = right atrium, *RV* = right ventricle.

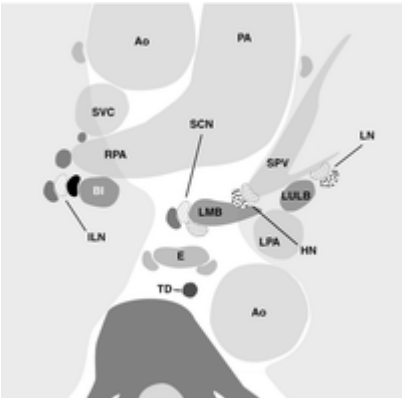

View larger version (30K):
[in this window]
[in a new window]
[Download PPT slide]

Figure 1c. Diagrams of the axial anatomy of the chest show the **lymph nodes** and drainage pathways for lung cancer in different lobes of the lung. All tumors drain to the interlobar and hilar **nodes**. The separate drainage pathways for tumors of the right upper lobe (black **nodes**), middle lobe (dark gray **nodes**), right lower lobe (striped **nodes**), left upper lobe (crosshatched **nodes**), and left lower lobe (dotted **nodes**) are shown. The corresponding American Thoracic Society (ATS) stations are labeled. ***E*** = esophagus, ***TD*** = thoracic duct. **(a)** Diagram shows the left paratracheal **nodes** *(LPTN)* (ATS station 2L) and right paratracheal **nodes** *(RPTN)* (ATS station 2R). *LBCV* = left brachiocephalic vein, *LCCA* = left common carotid artery, *LSCA* = left subclavian artery, *RBCA* = right brachiocephalic artery, *RBCV* = right brachiocephalic vein, *Tr* = trachea. **(b)** Diagram shows the left paratracheal **nodes** *(LPTN)* (ATS station 4L), right paratracheal **nodes** *(RPTN)* (ATS

station 4R), and subaortic **nodes** *(SAN)* (ATS station 5). *AA* = ascending aorta, *Ao* = aorta, *SVC* = superior vena cava, *Tr* = trachea. **(c)** Diagram shows the hilar **nodes** *(HN)* (ATS station 10), interlobar **nodes** *(ILN)* (ATS station 11), lobar **nodes** *(LN)* (ATS station 12), and subcarinal **nodes** *(SCN)* (ATS station 7). *Ao* = aorta, *BI* = bronchus intermedius, *LMB* = left main bronchus, *LPA* = left pulmonary artery, *LULB* = left upper lobe bronchus, *PA* = pulmonary artery, *RPA* = right pulmonary artery, *SPV* = superior pulmonary vein, *SVC* = superior vena cava. **(d)** Diagram shows the left inferior pulmonary ligament node *(LIPLN)* (ATS station 9) and right inferior pulmonary ligament node *(RIPLN)* (ATS station 9). *Ao* = aorta, *CS* = coronary sinus, *ECF* = epicardial fat, *LV* = left ventricle, *RA* = right atrium, *RV* = right ventricle.

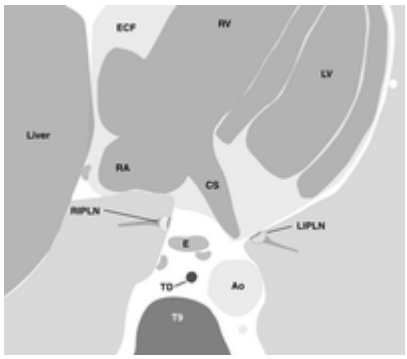

View larger version (25K):
[in this window]
[in a new window]
[Download PPT slide]

Figure 1d. Diagrams of the axial anatomy of the chest show the **lymph nodes** and drainage pathways for lung cancer in different lobes of the lung. All tumors drain to the interlobar and hilar **nodes**. The separate drainage pathways for tumors of the right upper lobe (black **nodes**), middle lobe (dark gray **nodes**), right lower lobe (striped **nodes**), left upper lobe (crosshatched **nodes**), and left lower lobe (dotted **nodes**) are shown. The corresponding American Thoracic Society (ATS) stations are labeled. ***E*** = esophagus, ***TD*** = thoracic duct. **(a)** Diagram shows the left paratracheal **nodes** *(LPTN)* (ATS station 2L) and right paratracheal **nodes** *(RPTN)* (ATS station 2R). *LBCV* = left brachiocephalic vein, *LCCA* = left common carotid artery, *LSCA* = left subclavian artery, *RBCA* = right brachiocephalic artery, *RBCV* = right brachiocephalic vein, *Tr* = trachea. **(b)** Diagram shows the left paratracheal **nodes** *(LPTN)* (ATS station 4L), right paratracheal **nodes** *(RPTN)* (ATS station 4R), and subaortic **nodes** *(SAN)* (ATS station 5). *AA* = ascending aorta, *Ao* = aorta, *SVC* = superior vena cava, *Tr* = trachea. **(c)** Diagram shows the hilar **nodes** *(HN)* (ATS station 10), interlobar **nodes** *(ILN)* (ATS station 11), lobar **nodes** *(LN)* (ATS station 12), and subcarinal **nodes** *(SCN)* (ATS station 7). *Ao* = aorta, *BI* = bronchus intermedius, *LMB* = left main bronchus, *LPA* = left pulmonary artery, *LULB* = left upper lobe bronchus, *PA* = pulmonary artery, *RPA* = right pulmonary artery, *SPV* = superior pulmonary vein, *SVC* = superior vena cava. **(d)** Diagram shows the left inferior pulmonary ligament node *(LIPLN)* (ATS station 9) and right inferior pulmonary ligament node *(RIPLN)* (ATS station 9). *Ao* = aorta, *CS* = coronary sinus, *ECF* = epicardial fat, *LV* = left ventricle, *RA* = right atrium, *RV* = right ventricle.

However, **mediastinal** metastases may occur through direct **lymph**atic drainage that

bypasses the hilar **nodes** (13,14). This is most commonly seen in the upper lobes. In rare instances, a direct connection may exist between the pulmonary segments and the thoracic duct, enabling direct passage of tumor into the systemic circulation without **mediastinal** node involvement (15).

In a patient with lung cancer, the nodal status determines surgical resectability. The TNM classification system for lung cancer (Table 1) (16) defines N1 disease as involvement of ipsilateral peribronchial, hilar, or intrapulmonary **nodes** (Fig 2). N1 **nodes** lie within the pleural reflection and correspond to ATS stations 10–14 (10). Cases of N1 disease are considered surgically resectable in the absence of **mediastinal** invasion by tumor, a malignant pleural effusion, satellite nodules, or metastases. Ipsilateral **mediastinal** or subcarinal node involvement is classified as N2 disease (Fig 3). These **nodes** lie outside the pleural reflection and correspond to ATS stations 1–9 (10). These cases may be amenable to surgery, but treatment also involves chemotherapy and irradiation. Contralateral **mediastinal** or hilar node involvement and disease in the supraclavicular **nodes** are classified as N3 disease (Fig 4). This is advanced disease, and patients are not surgical candidates.

View this table:
[in this window]
[in a new window]

TABLE 1. Nodal Staging in Lung Cancer according to the AJCC TNM Classification

View larger version (97K):
[in this window]
[in a new window]
[Download PPT slide]

Figure 2. Adenocarcinoma of the left upper lobe in a 60-year-old woman. CT scan shows a 3-cm-diameter left hilar node (ATS station 10) (arrow). At lobectomy, this node contained tumor tissue, whereas all other **nodes** were negative. This finding corresponds to N1 disease.

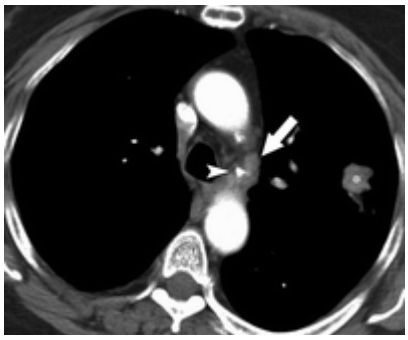

View larger version (78K):
[in this window]
[in a new window]
[Download PPT slide]

Figure 3. Adenocarcinoma of the left upper lobe in a 66-year-old man. CT scan obtained at the level of the aortopulmonary window shows a 7-mm-diameter subaortic node (ATS station 5) (arrow), which lies lateral to a calcified ligamentum arteriosum (arrowhead). The node contained tumor tissue at thoracotomy, a finding consistent with N2 disease. * = adenocarcinoma.

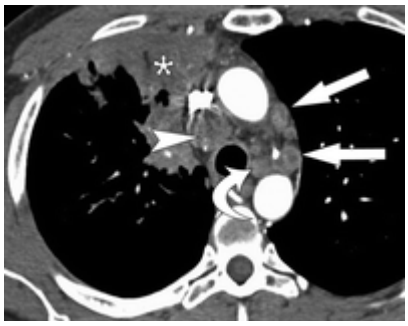

View larger version (87K):
[in this window]
[in a new window]
[Download PPT slide]

Figure 4. Adenocarcinoma of the right upper and middle lobes in a 35-year-old man. CT scan obtained at the level of the aortopulmonary window shows enhancing low right paratracheal **nodes** (ATS station 4R) (arrowhead), subaortic **nodes** (ATS station 5) (straight arrows), and low left (contralateral) paratracheal **nodes** (ATS station 4L) (curved arrow). The subaortic **nodes** contained tumor tissue at anterior parasternal mediastinotomy. Therefore, the patient has N3 disease, which is inoperable. * = adenocarcinoma.

CT is the most useful preoperative, noninvasive method of assessing for thoracic **lymph**adenopathy. However, nodal size cannot be used reliably to indicate metastatic involvement (7). McLoud et al (7) reported that 13% of **nodes** measuring less than 1 cm in evaluated patients with lung cancer were metastatic. Although the prevalence of metastatic disease increased with nodal size, one-third of **nodes** 2–4 cm in diameter were hyperplastic and did not contain metastases. A metaanalysis of 20 studies evaluated the accuracy of **mediastinal** staging for lung cancer with CT (5). Toloza et al (5) reported a pooled sensitivity for CT of 0.57 (95% confidence interval, 0.49–0.66) and specificity of 0.82 (95% confidence interval, 0.77–0.86). The overall positive predictive value and negative predictive value were 0.56 (range, 0.26–0.84) and 0.83 (range, 0.63–0.93), respectively.

The role of chest CT is to allow identification of enlarged **lymph nodes** and document their exact location so that an appropriate method for biopsy may be chosen, such as mediastinoscopy or fine-needle aspiration via a transbronchial, transesophageal, or transthoracic route.

Distinction between the different nodal stations around the right tracheobronchial angle can be difficult at CT, as the parietal pleural reflection is not visible (17). N1 **nodes** are within the confines of the pleural reflection and are therefore intrapulmonary. N2 **nodes** are outside the pleural reflection and are therefore **mediastinal**. The pleural reflection begins at the origin of the right upper lobe bronchus. **Lymph nodes** proximal to this bronchus should be considered **mediastinal** in location.

Magnetic resonance (MR) imaging is essentially equivalent to CT in staging, although Crisci et al (18) found that the administration of gadolinium contrast material improved staging accuracy. MR imaging is superior to CT in the evaluation of superior sulcus tumors for invasion of the brachial plexus or vertebral bodies.

FDG PET has shown significant improvement in radiologic staging of lung cancer. A metaanalysis of 18 studies (5) demonstrated a pooled sensitivity of 0.84 (95% confidence interval, 0.78–0.89) and specificity of 0.89 (95% confidence interval, 0.83–0.93). The overall positive predictive value and negative predictive value were 0.79 (range, 0.40–1.00) and 0.93 (range, 0.75–1.00), respectively. Because false-positive uptake of FDG can be seen with inflammatory and granulomatous diseases involving the **lymph nodes**, pathologic confirmation of **mediastinal** nodal involvement should be undertaken when there is increased uptake in **mediastinal lymph nodes** (5).

Breast Cancer

The breast and overlying skin are derived from the ectoderm and act as a single functional unit (19–21). The **lymph**atic drainage of the breast occurs through three principal routes: the axillary, transpectoral, and internal mammary pathways (22). According to Sappey (23), the skin, nipple, lactiferous tubules, and surrounding parenchyma drain into the subareolar plexus, which divides into medial and lateral trunks. The medial trunk receives **lymph** from the inferior breast. The lateral trunk receives **lymph** from the superior breast. These two trunks drain into the lower axillary **lymph nodes** (Fig 5). Studies by Tanis et al (20) also describe a direct route to the axilla, which may bypass the subareolar plexus.

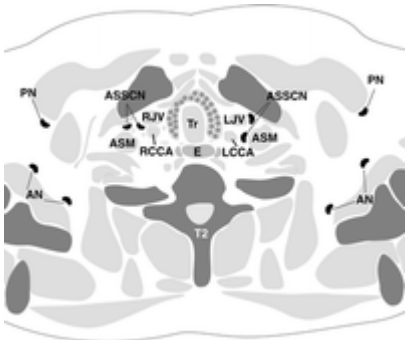

View larger version (42K):
[in this window]
[in a new window]
[Download PPT slide]

Figure 5a. Axial diagrams show the main drainage pathways (black **nodes**) of breast cancer to the axillary, internal mammary, and supraclavicular **lymph nodes**. ***E*** = esophagus, ***Tr*** = trachea. **(a)** Diagram shows the axillary **nodes** *(AN)*, anterior scalene/supraclavicular **nodes** *(ASSCN)*, and pectoral **nodes** *(PN)*. *ASM* = anterior scalene muscle, *LCCA* = left common carotid artery, *LJV* = left internal jugular vein, *RCCA* = right common carotid artery, *RJV* = right internal jugular vein. **(b)** Diagram shows the axillary **nodes** *(AN)*, pectoral **nodes** *(PN)*, and subclavian chain **nodes** *(SCCN)*. *LCCA* = left common carotid artery, *LJSCC* = left jugulosubclavian confluence, *LSCA* = left subclavian artery, *LSCV* = left subclavian vein, *RBCA* = right brachiocephalic artery, *RJSCC* = right jugulosubclavian confluence, *RSCV* = right subclavian vein, *TD* = thoracic duct. **(c)** Diagram shows the axillary **nodes** *(AN)*, internal mammary/retromanubrial **nodes** *(IMRMN)*, and pectoral **nodes** *(PN)*. *LBCV* = left brachiocephalic vein, *LCCA* = left common carotid artery, *LSCA* = left subclavian artery, *RBCA* = right brachiocephalic artery, *RBCV* = right brachiocephalic vein, *TD* = thoracic duct.

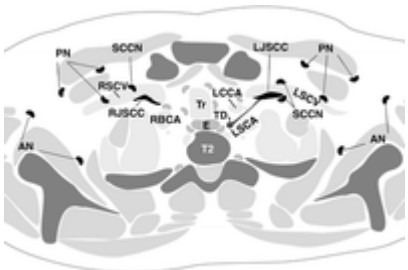

View larger version (40K):
[in this window]
[in a new window]
[Download PPT slide]

Figure 5b. Axial diagrams show the main drainage pathways (black **nodes**) of breast cancer to the axillary, internal mammary, and supraclavicular **lymph nodes**. ***E*** = esophagus, ***Tr*** = trachea. **(a)** Diagram shows the axillary **nodes** *(AN)*, anterior scalene/supraclavicular **nodes** *(ASSCN)*, and pectoral **nodes** *(PN)*. *ASM* = anterior scalene muscle, *LCCA* = left common carotid artery, *LJV* = left internal jugular vein, *RCCA* = right common carotid artery, *RJV* = right internal jugular vein. **(b)** Diagram shows the axillary **nodes** *(AN)*, pectoral **nodes** *(PN)*, and subclavian chain **nodes** *(SCCN)*. *LCCA* = left common carotid artery, *LJSCC* = left jugulosubclavian confluence, *LSCA* = left subclavian artery, *LSCV* = left subclavian vein, *RBCA* = right brachiocephalic artery, *RJSCC* = right jugulosubclavian confluence, *RSCV* = right subclavian vein, *TD* = thoracic duct. **(c)** Diagram shows the axillary **nodes** *(AN)*, internal mammary/retromanubrial **nodes** *(IMRMN)*, and pectoral **nodes** *(PN)*. *LBCV* = left brachiocephalic vein, *LCCA* = left common carotid artery, *LSCA* = left subclavian artery, *RBCA* = right brachiocephalic artery, *RBCV* = right brachiocephalic vein, *TD* = thoracic duct.

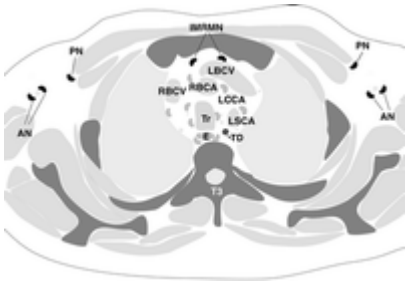

View larger version (37K):
[in this window]
[in a new window]
[Download PPT slide]

Figure 5c. Axial diagrams show the main drainage pathways (black **nodes**) of breast cancer to the axillary, internal mammary, and supraclavicular **lymph nodes**. ***E*** = esophagus, ***Tr*** = trachea. **(a)** Diagram shows the axillary **nodes** *(AN)*, anterior scalene/supraclavicular **nodes** *(ASSCN)*, and pectoral **nodes** *(PN)*. *ASM* = anterior scalene muscle, *LCCA* = left common carotid artery, *LJV* = left internal jugular vein, *RCCA* = right common carotid artery, *RJV* = right internal jugular vein. **(b)** Diagram shows the axillary **nodes** *(AN)*, pectoral **nodes** *(PN)*, and subclavian chain **nodes** *(SCCN)*. *LCCA* = left common carotid artery, *LJSCC* = left jugulosubclavian confluence, *LSCA* = left subclavian artery, *LSCV* = left subclavian vein, *RBCA* = right brachiocephalic artery, *RJSCC* = right jugulosubclavian confluence, *RSCV* = right subclavian vein, *TD* = thoracic duct. **(c)** Diagram shows the axillary **nodes** *(AN)*, internal mammary/retromanubrial **nodes** *(IMRMN)*, and pectoral **nodes** *(PN)*. *LBCV* = left brachiocephalic vein, *LCCA* = left common carotid artery, *LSCA* = left subclavian artery, *RBCA* = right brachiocephalic artery, *RBCV* = right brachiocephalic vein, *TD* = thoracic duct.

The axillary **lymph nodes** are divided into three levels with respect to their position relative to the pectoralis minor muscle (16) (Fig 6). Level I **nodes**, or low axillary **nodes**, lie lateral to the

lateral border of the pectoralis minor. Level II **nodes** lie between the medial and lateral borders of the pectoralis minor and include the interpectoral **nodes** of Rotter (Fig 7). Level III **nodes** are the highest group and lie medial to the medial margin of the pectoralis minor. Intramammary **nodes**, or **nodes** within the breast parenchyma, are regarded as axillary **nodes** for staging purposes. The axillary **nodes** drain into **lymph**atics that course along the axillary and contiguous subclavian vein. From here, the **lymph**atics may drain directly into the jugulosubclavian confluence or initially pass through the jugular and broncho**mediastinal** **lymph**atics.

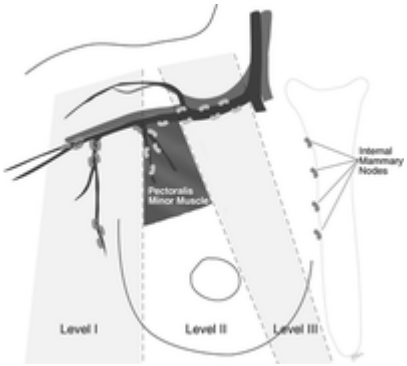

View larger version (38K):
[in this window]
[in a new window]
[Download PPT slide]

Figure 6. Diagram shows the **lymph**atic drainage of the right breast. The axillary **nodes** are divided into three levels according to their positions relative to the pectoralis minor muscle.

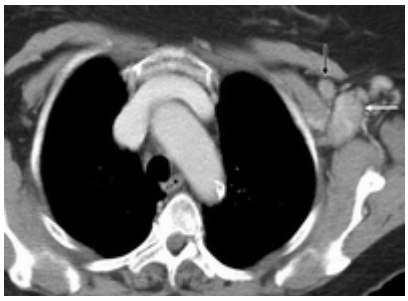

View larger version (113K):
[in this window]
[in a new window]
[Download PPT slide]

Figure 7. Metastatic breast cancer in a 68-year-old woman. CT scan obtained at the level of the aortic arch shows enlarged left axillary **nodes** that are located lateral to the pectoralis minor muscle (level I) (white arrow) and within the interpectoral space (level II) (black arrow). The **nodes** contained tumor tissue, a finding defined as N1 disease.

The **lymph**atics that drain the medial breast perforate the pectoral and intercostal muscles and enter the internal mammary **lymph nodes** (Fig 8). The internal mammary **nodes** and **lymph**atics lie in the intercostal spaces along the margins of the sternum and are usually present from the fifth intercostal space to the clavicles. Rarely, the breast parenchyma may drain directly into the supraclavicular **nodes**. When tumor obstructs normal **lymph**atic flow, collateral pathways open. These include contralateral internal mammary and **mediastinal** **lymph**atics. Spread through the rectus abdominus muscle sheath to the subdiaphragmatic and subperitoneal plexus may lead to spread to the liver and retroperitoneal **nodes**.

View larger version (91K):
[in this window]
[in a new window]
[Download PPT slide]

Figure 8. Breast cancer in a 72-year-old woman. CT scan obtained at the level of the great vessels shows multiple left subpectoral **nodes** (level II) (white arrow), a left internal mammary node (black arrow), and a right paratracheal node (arrowhead). A left pleural effusion and multiple pulmonary metastases are also present. These findings are defined as stage IV disease due to the pulmonary metastases.

In patients with breast cancer, **lymph** node status is one of the most important prognostic factors (16). The TNM staging system for breast cancer (Table 2) classifies mobile axillary **nodes** as N1. The confirmation of N1 disease requires chemotherapy and/or hormone therapy in addition to surgery. Axillary **nodes** that are fixed to each other or to adjacent structures are classified as N2. The confirmation of N2 disease requires chemotherapy and radiation therapy in addition to surgery. Further subdivisions depend on the number of positive axillary **nodes**. Isolated ipsilateral internal mammary nodal disease is defined as N2. If both the axillary and internal mammary **nodes** are involved, this is defined as N3 (16). Disease involving infraclavicular and supraclavicular **nodes** is also defined as N3. Preoperative chemotherapy is necessary in cases of N3 disease.

View this table:
[in this window]
[in a new window]

TABLE 2. Nodal Staging in Breast Cancer according to the AJCC TNM Classification

In patients with small tumors and clinically negative axillae, preoperative sentinel node imaging is useful in limiting the extent of surgical intervention (24–26). This node can be imaged by injecting technetium-99m radiocolloid or blue dye into or adjacent to the tumor (21). The first draining axillary node or sentinel node is identified and resected. If this node is free of tumor, further dissection is not performed.

CT does not currently have a role in the preoperative staging of every patient with newly diagnosed breast cancer. The sensitivity of CT for axillary metastases is reported as only 50%–60% (27,28). CT is used in the assessment of a patient with a large tumor or with palpable, fixed axillary **nodes**, where there is high suspicion of occult metastatic disease.

Improved accuracy has been achieved by using thin-section CT in patients lying prone (29). CT identification of the sentinel **lymph** node has also shown good correlation with dye- and gamma probe–guided sentinel **lymph** node biopsy (30). This is defined at CT as the most inferior **lymph** node adjacent to the lateral thoracic vessels.

Lymphoma

The **lymph**omas are a diverse group of neoplastic disorders. They are divided into Hodgkin disease (characterized by the presence of Reed-Sternberg cells) and non-Hodgkin **lymph**oma. Further subdivisions depend on the histologic type. A number of pathologic classifications have been described. The most updated and widely used classification is the combined Revised European-American Classification of **Lymph**oid Neoplasms (REAL)/World Health Organization Classification of **Lymph**oid Neoplasms (31).

More than 80% of patients with Hodgkin disease have intrathoracic involvement at initial presentation (32). In the thorax, Hodgkin disease most frequently involves the anterior **mediastinal** and paratracheal regions (Fig 9) and tends to spread to contiguous nodal groups. The subcarinal, peridiaphragmatic, periesophageal, and internal mammary **nodes** are involved in decreasing order of frequency. In most patients, two or more nodal groups are involved at initial presentation. Isolated hilar involvement is rare and should suggest an alternative diagnosis.

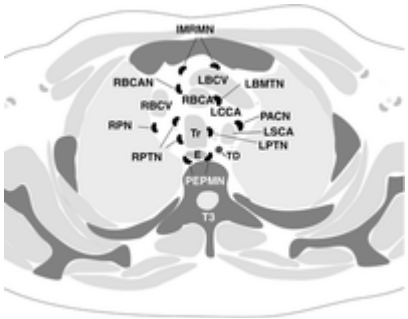

View larger version (43K):
[in this window]
[in a new window]
[Download PPT slide]

Figure 9a. Axial diagrams show the main intrathoracic drainage pathways (black **nodes**) for **lymph**oma. ***E*** = esophagus, ***TD*** = thoracic duct. **(a)** Diagram shows the internal mammary/retromanubrial **nodes** *(IMRMN)*, left bronchomediastinal trunk node *(LBMTN)*, left paratracheal node *(LPTN)*, preaortocarotid node *(PACN)*, periesophageal/posterior mediastinum **nodes** *(PEPMN)*, right brachiocephalic angle node *(RBCAN)*, right phrenic node *(RPN)*, and right paratracheal **nodes** *(RPTN)*. *LBCV* = left brachiocephalic vein, *LCCA* = left common carotid artery, *LSCA* = left subclavian artery, *RBCA* = right brachiocephalic artery, *RBCV* = right brachiocephalic vein, *Tr* = trachea. **(b)** Diagram shows the internal mammary **nodes** *(IMN)*, left phrenic node *(LPN)*, periesophageal/posterior mediastinum **nodes** *(PEPMN)*, right phrenic node *(RPN)*, and right paratracheal **nodes** *(RPTN)*. *AA* = aortic arch, *LBCV* = left brachiocephalic vein, *RBCV* = right brachiocephalic vein, *Tr* = trachea. **(c)** Diagram shows the extrapleural **nodes** *(EPN)*, internal mammary **nodes** *(IMN)*, lobar node *(LN)*, left phrenic node *(LPN)*, periesophageal/posterior mediastinum **nodes** *(PEPMN)*, subcarinal node *(SCN)*, and segmental node *(SN)*. *AA* = ascending aorta, *Ao* = aorta, *LMB* = left main bronchus, *PA* = pulmonary artery, *RMB* = right main bronchus, *RPA* = right pulmonary artery, *SVC* = superior vena cava. **(d)** Diagram shows the pericardial fat **nodes** *(PCFN)* and periesophageal/posterior mediastinum **nodes** *(PEPMN)*. *Ao* = aorta, *CS* = coronary sinus, *ECF* = epicardial fat, *LV* = left ventricle, *PCF* = pericardial fat, *RA* = right atrium, *RV* = right ventricle. **(e)** Diagram shows the anterior peridiaphragmatic

nodes *(APDN)*, extrapleural **nodes** *(EPN)*, gastrohepatic ligament/celiac **nodes** *(GHLCN)*, and periesophageal/posterior mediastinum **nodes** *(PEPMN)*. *Ao* = aorta.

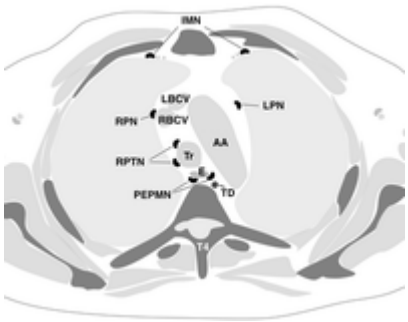

View larger version (36K):
[in this window]
[in a new window]
[Download PPT slide]

Figure 9b. Axial diagrams show the main intrathoracic drainage pathways (black **nodes**) for **lymph**oma. ***E*** = esophagus, ***TD*** = thoracic duct. **(a)** Diagram shows the internal mammary/retromanubrial **nodes** *(IMRMN)*, left broncho**mediastinal** trunk node *(LBMTN)*, left paratracheal node *(LPTN)*, preaortocarotid node *(PACN)*, periesophageal/posterior mediastinum **nodes** *(PEPMN)*, right brachiocephalic angle node *(RBCAN)*, right phrenic node *(RPN)*, and right paratracheal **nodes** *(RPTN)*. *LBCV* = left brachiocephalic vein, *LCCA* = left common carotid artery, *LSCA* = left subclavian artery, *RBCA* = right brachiocephalic artery, *RBCV* = right brachiocephalic vein, *Tr* = trachea. **(b)** Diagram shows the internal mammary **nodes** *(IMN)*, left phrenic node *(LPN)*, periesophageal/posterior mediastinum **nodes** *(PEPMN)*, right phrenic node *(RPN)*, and right paratracheal **nodes** *(RPTN)*. *AA* = aortic arch, *LBCV* = left brachiocephalic vein, *RBCV* = right brachiocephalic vein, *Tr* = trachea. **(c)** Diagram shows the extrapleural **nodes** *(EPN)*, internal mammary **nodes** *(IMN)*, lobar node *(LN)*, left phrenic node *(LPN)*, periesophageal/posterior mediastinum **nodes** *(PEPMN)*, subcarinal node *(SCN)*, and segmental node *(SN)*. *AA* = ascending aorta, *Ao* = aorta, *LMB* = left main bronchus, *PA* = pulmonary artery, *RMB* = right main bronchus, *RPA* = right pulmonary artery, *SVC* = superior vena cava. **(d)** Diagram shows the pericardial fat **nodes** *(PCFN)* and periesophageal/posterior mediastinum **nodes** *(PEPMN)*. *Ao* = aorta, *CS* = coronary sinus, *ECF* = epicardial fat, *LV* = left ventricle, *PCF* = pericardial fat, *RA* = right atrium, *RV* = right ventricle. **(e)** Diagram shows the anterior peridiaphragmatic **nodes** *(APDN)*, extrapleural **nodes** *(EPN)*, gastrohepatic ligament/celiac **nodes** *(GHLCN)*, and periesophageal/posterior mediastinum **nodes** *(PEPMN)*. *Ao* = aorta.

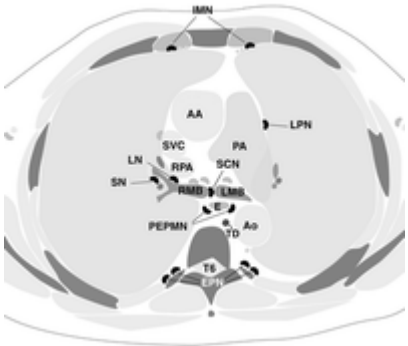

View larger version (41K):
[in this window]
[in a new window]
[Download PPT slide]

Figure 9c. Axial diagrams show the main intrathoracic drainage pathways (black **nodes**) for **lymph**oma. ***E*** = esophagus, ***TD*** = thoracic duct. **(a)** Diagram shows the internal mammary/retromanubrial **nodes** *(IMRMN)*, left broncho**mediastinal** trunk node *(LBMTN)*, left paratracheal node *(LPTN)*, preaortocarotid node *(PACN)*, periesophageal/posterior mediastinum **nodes** *(PEPMN)*, right brachiocephalic angle node *(RBCAN)*, right phrenic node *(RPN)*, and right paratracheal **nodes** *(RPTN)*. *LBCV* = left brachiocephalic vein, *LCCA* = left common carotid artery, *LSCA* = left subclavian artery, *RBCA* = right brachiocephalic artery, *RBCV* = right brachiocephalic vein, *Tr* = trachea. **(b)** Diagram shows the internal mammary **nodes** *(IMN)*, left phrenic node *(LPN)*, periesophageal/posterior mediastinum **nodes** *(PEPMN)*, right phrenic node *(RPN)*, and right paratracheal **nodes** *(RPTN)*. *AA* = aortic arch, *LBCV* = left brachiocephalic vein, *RBCV* = right brachiocephalic vein, *Tr* = trachea. **(c)** Diagram shows the extrapleural **nodes** *(EPN)*, internal mammary **nodes** *(IMN)*, lobar node *(LN)*, left phrenic node *(LPN)*, periesophageal/posterior mediastinum **nodes** *(PEPMN)*, subcarinal node *(SCN)*, and segmental node *(SN)*. *AA* = ascending aorta, *Ao* = aorta, *LMB* = left main bronchus, *PA* = pulmonary artery, *RMB* = right main bronchus, *RPA* = right pulmonary artery, *SVC* = superior vena cava. **(d)** Diagram shows the pericardial fat **nodes** *(PCFN)* and periesophageal/posterior mediastinum **nodes** *(PEPMN)*. *Ao* = aorta, *CS* = coronary sinus, *ECF* = epicardial fat, *LV* = left ventricle, *PCF* = pericardial fat, *RA* = right atrium, *RV* = right ventricle. **(e)** Diagram shows the anterior peridiaphragmatic **nodes** *(APDN)*, extrapleural **nodes** *(EPN)*, gastrohepatic ligament/celiac **nodes** *(GHLCN)*, and periesophageal/posterior mediastinum **nodes** *(PEPMN)*. *Ao* = aorta.

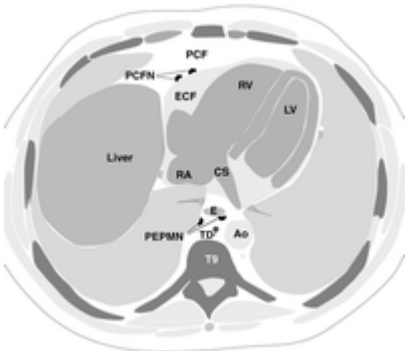

View larger version (42K):
[in this window]
[in a new window]
[Download PPT slide]

Figure 9d. Axial diagrams show the main intrathoracic drainage pathways (black **nodes**) for **lymph**oma. ***E*** = esophagus, ***TD*** = thoracic duct. **(a)** Diagram shows the internal mammary/retromanubrial **nodes** *(IMRMN)*, left broncho**mediastinal** trunk node *(LBMTN)*, left paratracheal node *(LPTN)*, preaortocarotid node *(PACN)*, periesophageal/posterior mediastinum **nodes** *(PEPMN)*, right brachiocephalic angle node *(RBCAN)*, right phrenic node *(RPN)*, and right paratracheal **nodes** *(RPTN)*. *LBCV* = left brachiocephalic vein, *LCCA* = left common carotid artery, *LSCA* = left subclavian artery, *RBCA* = right brachiocephalic artery, *RBCV* = right brachiocephalic vein, *Tr* = trachea. **(b)** Diagram shows the internal mammary **nodes** *(IMN)*, left phrenic node *(LPN)*, periesophageal/posterior

mediastinum **nodes** *(PEPMN)*, right phrenic node *(RPN)*, and right paratracheal **nodes** *(RPTN)*. *AA* = aortic arch, *LBCV* = left brachiocephalic vein, *RBCV* = right brachiocephalic vein, *Tr* = trachea. **(c)** Diagram shows the extrapleural **nodes** *(EPN)*, internal mammary **nodes** *(IMN)*, lobar node *(LN)*, left phrenic node *(LPN)*, periesophageal/posterior mediastinum **nodes** *(PEPMN)*, subcarinal node *(SCN)*, and segmental node *(SN)*. *AA* = ascending aorta, *Ao* = aorta, *LMB* = left main bronchus, *PA* = pulmonary artery, *RMB* = right main bronchus, *RPA* = right pulmonary artery, *SVC* = superior vena cava. **(d)** Diagram shows the pericardial fat **nodes** *(PCFN)* and periesophageal/posterior mediastinum **nodes** *(PEPMN)*. *Ao* = aorta, *CS* = coronary sinus, *ECF* = epicardial fat, *LV* = left ventricle, *PCF* = pericardial fat, *RA* = right atrium, *RV* = right ventricle. **(e)** Diagram shows the anterior peridiaphragmatic **nodes** *(APDN)*, extrapleural **nodes** *(EPN)*, gastrohepatic ligament/celiac **nodes** *(GHLCN)*, and periesophageal/posterior mediastinum **nodes** *(PEPMN)*. *Ao* = aorta.

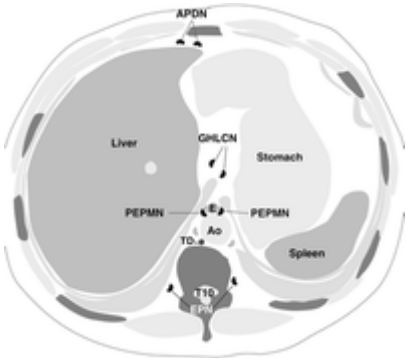

View larger version (40K):
[in this window]
[in a new window]
[Download PPT slide]

Figure 9e. Axial diagrams show the main intrathoracic drainage pathways (black **nodes**) for **lymph**oma. ***E*** = esophagus, ***TD*** = thoracic duct. **(a)** Diagram shows the internal mammary/retromanubrial **nodes** *(IMRMN)*, left broncho**mediastinal** trunk node *(LBMTN)*, left paratracheal node *(LPTN)*, preaortocarotid node *(PACN)*, periesophageal/posterior mediastinum **nodes** *(PEPMN)*, right brachiocephalic angle node *(RBCAN)*, right phrenic node *(RPN)*, and right paratracheal **nodes** *(RPTN)*. *LBCV* = left brachiocephalic vein, *LCCA* = left common carotid artery, *LSCA* = left subclavian artery, *RBCA* = right brachiocephalic artery, *RBCV* = right brachiocephalic vein, *Tr* = trachea. **(b)** Diagram shows the internal mammary **nodes** *(IMN)*, left phrenic node *(LPN)*, periesophageal/posterior mediastinum **nodes** *(PEPMN)*, right phrenic node *(RPN)*, and right paratracheal **nodes** *(RPTN)*. *AA* = aortic arch, *LBCV* = left brachiocephalic vein, *RBCV* = right brachiocephalic vein, *Tr* = trachea. **(c)** Diagram shows the extrapleural **nodes** *(EPN)*, internal mammary **nodes** *(IMN)*, lobar node *(LN)*, left phrenic node *(LPN)*, periesophageal/posterior mediastinum **nodes** *(PEPMN)*, subcarinal node *(SCN)*, and segmental node *(SN)*. *AA* = ascending aorta, *Ao* = aorta, *LMB* = left main bronchus, *PA* = pulmonary artery, *RMB* = right main bronchus, *RPA* = right pulmonary artery, *SVC* = superior vena cava. **(d)** Diagram shows the pericardial fat **nodes** *(PCFN)* and periesophageal/posterior mediastinum **nodes** *(PEPMN)*. *Ao* = aorta, *CS* = coronary sinus, *ECF* = epicardial fat, *LV* = left ventricle, *PCF* = pericardial fat, *RA* = right atrium, *RV* = right ventricle. **(e)**

Diagram shows the anterior peridiaphragmatic **nodes** *(APDN)*, extrapleural **nodes** *(EPN)*, gastrohepatic ligament/celiac **nodes** *(GHLCN)*, and periesophageal/posterior mediastinum **nodes** *(PEPMN)*. *Ao* = aorta.

Non-Hodgkin **lymph**oma is a more heterogeneous group of diseases, and thoracic involvement is present in up to 45% of cases (33). It is difficult to differentiate Hodgkin disease from non-Hodgkin **lymph**oma on the basis of nodal distribution alone. The paratracheal and anterior **mediastinal nodes** are still the most common sites of involvement for non-Hodgkin **lymph**oma (Fig 10). Other common sites, in decreasing order of frequency, are the subcarinal, hilar (Fig 10), posterior **mediastinal** (paraaortic, paravertebral, and retrocrural), and pericardial **nodes** (33).

View larger version (85K):
[in this window]
[in a new window]
[Download PPT slide]

Figure 10a. Non-Hodgkin **lymph**oma in a 66-year-old man. **(a)** CT scan obtained at the level of the great vessels shows bilateral axillary, right paratracheal (white arrow), left internal mammary (black arrow), and anterior **mediastinal** (arrowhead) **nodes**. **(b)** CT scan obtained at the level of the main pulmonary artery shows a left internal mammary node. Right hilar (arrow) and subcarinal (arrowhead) **lymph**adenopathy and bilateral pleural effusions are also present. **(c)** CT scan obtained at the level of the interventricular septum shows enlarged pericardial fat **nodes** (black arrow). Soft tissue in the extrapleural space (white arrows) and bilateral pleural effusions are also present.

View larger version (90K):
[in this window]
[in a new window]
[Download PPT slide]

Figure 10b. Non-Hodgkin **lymph**oma in a 66-year-old man. **(a)** CT scan obtained at the level of the great vessels shows bilateral axillary, right paratracheal (white arrow), left internal mammary (black arrow), and anterior **mediastinal** (arrowhead) **nodes**. **(b)** CT scan obtained at the level of the main pulmonary artery shows a left internal mammary node. Right hilar (arrow) and subcarinal (arrowhead) **lymph**adenopathy and bilateral pleural effusions are also present. **(c)** CT scan obtained at the level of the interventricular septum shows enlarged pericardial fat **nodes** (black arrow). Soft tissue in the extrapleural space (white arrows) and bilateral pleural effusions are also present.

View larger version (110K):
[in this window]
[in a new window]
[Download PPT slide]

Figure 10c. Non-Hodgkin **lymph**oma in a 66-year-old man. **(a)** CT scan obtained at the level of the great vessels shows bilateral axillary, right paratracheal (white arrow), left internal mammary (black arrow), and anterior **mediastinal** (arrowhead) **nodes**. **(b)** CT scan obtained at the level of the main pulmonary artery shows a left internal mammary node. Right hilar (arrow) and subcarinal (arrowhead) **lymph**adenopathy and bilateral pleural effusions are also present. **(c)** CT scan obtained at the level of the interventricular septum shows enlarged pericardial fat **nodes** (black arrow). Soft tissue in the extrapleural space (white arrows) and bilateral pleural effusions are also present.

Histopathologic classification and tumor size are the most important prognostic factors for non-Hodgkin **lymph**oma. In both Hodgkin disease and non-Hodgkin **lymph**oma, single-station nodal disease is defined as stage 1. Multiple **nodes** confined to one body area such as the chest are defined as stage 2, and disease on both sides of the diaphragm is defined as stage 3. Visceral involvement is regarded as stage 4. The grade and bulk of tumor determine whether treatment is with chemotherapy, radiation therapy, or a combination. Accurate description of the extent of disease is important for radiation therapy planning. Large **mediastinal** adenopathy or bulky disease is defined as the presence of a **mediastinal** mass greater than 10 cm in transverse diameter or greater than one-third of the thoracic diameter (measured at the level of the diaphragm). Large **mediastinal** adenopathy is associated with an increased risk of relapse and therefore requires both chemotherapy and radiation therapy, regardless of tumor grade (16).

Recurrent disease is common in the pericardial and internal mammary **lymph nodes**, as these are usually not included in the radiation field. Involvement of the posterior **mediastinal lymph nodes** is associated with pleural, retrocrural, and retroperitoneal disease (Fig 10). Nodal disease can also occur in the extrapleural space, especially in patients with non-Hodgkin **lymph**oma (34). There is often an associated pleural effusion secondary to malignancy or obstruction of the pleural **lymph**atics. **Lymph** node calcification before treatment is unusual (0.84% of cases) but has been associated with aggressive Hodgkin disease or non-Hodgkin **lymph**oma (35). After treatment, diseased **lymph nodes** may show irregular or eggshell calcifications at CT.

Esophageal Carcinoma

The esophagus is divided into cervical and thoracic portions. The cervical esophagus begins at the level of the lower margin of the cricoid cartilage and ends at the thoracic inlet. The thoracic esophagus extends from the thoracic inlet to the gastroesophageal junction and is divided into three regions (36). The upper thoracic portion extends from the thoracic inlet (at the level of the suprasternal notch) to the carina. The midthoracic portion extends from the carina to just above the gastroesophageal junction. The lower esophagus includes the intraabdominal esophagus and the gastroesophageal junction.

The esophageal **lymph**atics form an uninterrupted dense submucosal plexus around the esophagus (37,38). In general, the **lymph**atics of the upper two-thirds of the esophagus drain cephalad. The **lymph**atics of the lower one-third drain caudally toward the abdomen. Esophageal **lymph**atics also directly communicate with the neighboring thoracic duct at

multiple levels. As a result of this extensive drainage system, skip metastases are common, whereby nodal disease appears at remote sites with no intervening nodal involvement (37). Nodal spread of tumors from the upper and middle esophagus often involves paratracheal **lymph nodes**. The most frequent sites of nodal spread for lower esophageal cancers are the **lymph nodes** of the lesser curvature and left gastric artery (gastrohepatic ligament **nodes**).

Nodal spread of esophageal tumors may be extensive at initial clinical presentation (Fig 11). The TNM staging system for esophageal cancer (Table 3) reflects the bidirectional longitudinal **lymph**atic flow along the esophagus. It is essential to evaluate the entire thorax from the thoracic inlet to the upper abdomen (Fig 12) in all patients with esophageal carcinoma because the detection and confirmation of regional nodal disease necessitates the addition of chemoradiation treatment to surgery. The specific regional **nodes** for tumors of the cervical esophagus include the supraclavicular, internal jugular, upper and lower cervical, and periesophageal **nodes**. Regional **nodes** for tumors of the thoracic esophagus are the paratracheal, periesophageal, and subcarinal **nodes** (below the azygos vein). For gastroesophageal junction tumors, the regional **nodes** include **nodes** adjacent to the diaphragm, pericardium, left gastric artery (gastrohepatic ligament), and celiac artery (16). For all intrathoracic esophageal tumors, supraclavicular and celiac axis nodal involvement is classified as distant metastatic disease (16) and precludes surgery.

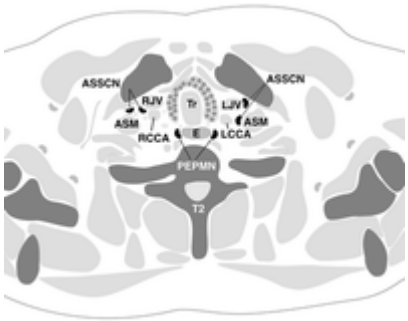

View larger version (39K):
[in this window]
[in a new window]
[Download PPT slide]

Figure 11a. Axial diagrams show the regional drainage pathways (black **nodes**) for esophageal cancer. Supraclavicular **nodes** are considered regional **nodes** (N1) for tumors that originate at the cervical esophagus but represent distant disease (M1) for intrathoracic esophageal tumors. ***E*** = esophagus. **(a)** Diagram shows the anterior scalene/supraclavicular **nodes** *(ASSCN)* and periesophageal/posterior mediastinum **nodes** *(PEPMN)*. *ASM* = anterior scalene muscle, *LCCA* = left common carotid artery, *LJV* = left internal jugular vein, *RCCA* = right common carotid artery, *RJV* = right internal jugular vein, *Tr* = trachea. **(b)** Diagram shows the periesophageal/posterior mediastinum **nodes** *(PEPMN)* and right paratracheal **nodes** *(RPTN)*. *AA* = aortic arch, *LBCV* = left brachiocephalic vein, *RBCV* = right brachiocephalic vein, *TD* = thoracic duct, *Tr* = trachea. **(c)** Diagram shows the periesophageal/posterior mediastinum **nodes** *(PEPMN)* and subcarinal node *(SCN)*. *AA* = ascending aorta, *Ao* = aorta, *LMB* = left main bronchus, *PA* = pulmonary artery, *RMB* = right main bronchus, *RPA* = right pulmonary artery, *SVC* = superior vena cava, *TD* = thoracic duct. **(d)** Diagram shows the gastrohepatic ligament/celiac **nodes** *(GHLCN)* and periesophageal/posterior mediastinum **nodes** *(PEPMN)*. *Ao* = aorta, *TD* = thoracic duct.

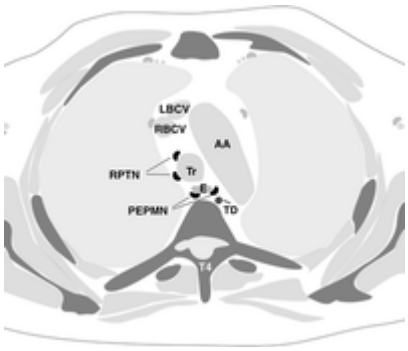

View larger version (37K):
[in this window]
[in a new window]
[Download PPT slide]

Figure 11b. Axial diagrams show the regional drainage pathways (black **nodes**) for esophageal cancer. Supraclavicular **nodes** are considered regional **nodes** (N1) for tumors that originate at the cervical esophagus but represent distant disease (M1) for intrathoracic esophageal tumors. ***E*** = esophagus. **(a)** Diagram shows the anterior scalene/supraclavicular **nodes** *(ASSCN)* and periesophageal/posterior mediastinum **nodes** *(PEPMN)*. *ASM* = anterior scalene muscle, *LCCA* = left common carotid artery, *LJV* = left internal jugular vein, *RCCA* = right common carotid artery, *RJV* = right internal jugular vein, *Tr* = trachea. **(b)** Diagram shows the periesophageal/posterior mediastinum **nodes** *(PEPMN)* and right paratracheal **nodes** *(RPTN)*. *AA* = aortic arch, *LBCV* = left brachiocephalic vein, *RBCV* = right brachiocephalic vein, *TD* = thoracic duct, *Tr* = trachea. **(c)** Diagram shows the periesophageal/posterior mediastinum **nodes** *(PEPMN)* and subcarinal node *(SCN)*. *AA* = ascending aorta, *Ao* = aorta, *LMB* = left main bronchus, *PA* = pulmonary artery, *RMB* = right main bronchus, *RPA* = right pulmonary artery, *SVC* = superior vena cava, *TD* = thoracic duct. **(d)** Diagram shows the gastrohepatic ligament/celiac **nodes** *(GHLCN)* and periesophageal/posterior mediastinum **nodes** *(PEPMN)*. *Ao* = aorta, *TD* = thoracic duct.

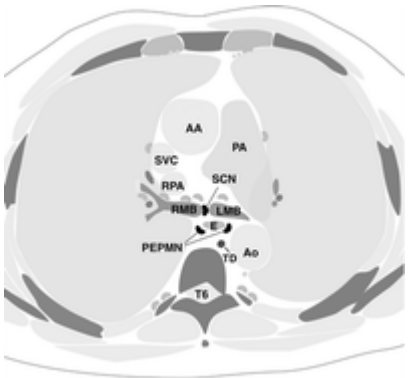

View larger version (40K):
[in this window]
[in a new window]
[Download PPT slide]

Figure 11c. Axial diagrams show the regional drainage pathways (black **nodes**) for esophageal cancer. Supraclavicular **nodes** are considered regional **nodes** (N1) for tumors that originate at the cervical esophagus but represent distant disease (M1) for intrathoracic esophageal tumors. ***E*** = esophagus. **(a)** Diagram shows the anterior scalene/supraclavicular **nodes** *(ASSCN)* and periesophageal/posterior mediastinum **nodes** *(PEPMN)*. *ASM* = anterior scalene muscle, *LCCA* = left common carotid artery, *LJV* = left internal jugular vein, *RCCA* = right common carotid artery, *RJV* = right internal jugular vein, *Tr* = trachea. **(b)** Diagram shows the periesophageal/posterior mediastinum **nodes** *(PEPMN)* and right paratracheal **nodes** *(RPTN)*. *AA* = aortic arch, *LBCV* = left brachiocephalic vein, *RBCV* = right brachiocephalic vein, *TD* = thoracic duct, *Tr* = trachea. **(c)** Diagram shows the periesophageal/posterior mediastinum **nodes** *(PEPMN)* and subcarinal node *(SCN)*. *AA* = ascending aorta, *Ao* = aorta, *LMB* = left main bronchus, *PA* = pulmonary artery, *RMB* = right main bronchus, *RPA* = right pulmonary artery, *SVC* = superior vena cava, *TD* = thoracic duct. **(d)** Diagram shows the gastrohepatic ligament/celiac **nodes** *(GHLCN)* and periesophageal/posterior mediastinum **nodes** *(PEPMN)*. *Ao* = aorta, *TD* = thoracic duct.

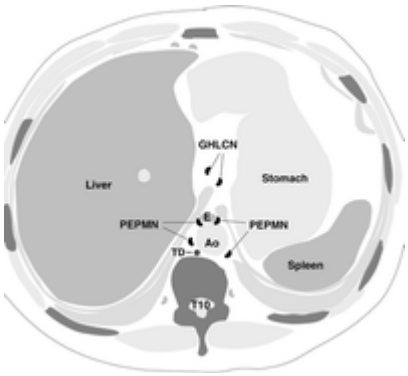

View larger version (39K):
[in this window]
[in a new window]
[Download PPT slide]

Figure 11d. Axial diagrams show the regional drainage pathways (black **nodes**) for esophageal cancer. Supraclavicular **nodes** are considered regional **nodes** (N1) for tumors that originate at the cervical esophagus but represent distant disease (M1) for intrathoracic esophageal tumors. ***E*** = esophagus. **(a)** Diagram shows the anterior scalene/supraclavicular **nodes** *(ASSCN)* and periesophageal/posterior mediastinum **nodes** *(PEPMN)*. *ASM* = anterior scalene muscle, *LCCA* = left common carotid artery, *LJV* = left internal jugular vein, *RCCA* = right common carotid artery, *RJV* = right internal jugular vein, *Tr* = trachea. **(b)** Diagram shows the periesophageal/posterior mediastinum **nodes** *(PEPMN)* and right paratracheal **nodes** *(RPTN)*. *AA* = aortic arch, *LBCV* = left brachiocephalic vein, *RBCV* = right brachiocephalic vein, *TD* = thoracic duct, *Tr* = trachea. **(c)** Diagram shows the periesophageal/posterior mediastinum **nodes** *(PEPMN)* and subcarinal node *(SCN)*. *AA* = ascending aorta, *Ao* = aorta, *LMB* = left main bronchus, *PA* = pulmonary artery, *RMB* = right main bronchus, *RPA* = right pulmonary artery, *SVC* = superior vena cava, *TD* = thoracic duct. **(d)** Diagram shows the gastrohepatic ligament/celiac **nodes** *(GHLCN)* and periesophageal/posterior mediastinum **nodes** *(PEPMN)*. *Ao* = aorta, *TD* = thoracic duct.

View this table:
[in this window]
[in a new window]

TABLE 3. Nodal Staging in Esophageal Cancer according to the AJCC TNM Classification

View larger version (158K):
[in this window]
[in a new window]
[Download PPT slide]

Figure 12. Lower esophageal carcinoma in a 71-year-old man. CT scan obtained at the level of the falciform ligament shows several gastrohepatic ligament **nodes** (arrow), which contained tumor tissue. These **nodes** are defined as distant disease for intrathoracic esophageal tumors but as regional **nodes** for tumors that originate at the gastroesophageal junction.

Studies of normal **lymph** node size have found that normal paraesophageal **nodes** measure up to 1 cm in diameter (3). However, more recent data suggest that this is an overestimation. Schroder et al (39) performed a histopathologic study of **lymph**adenectomy specimens from patients with esophageal carcinoma. They analyzed a total of 1,196 **lymph nodes**, of which 129 (10.8%) were malignant, and found no significant correlation between **lymph** node size and the frequency of nodal metastases. The average size of nonmetastatic **nodes** was 5 mm. The average size of metastatic **lymph nodes** was 6.7 mm, and only 12% of metastatic **nodes** were greater than 10 mm in diameter. Dhar et al (40) reported that patients with metastatic **lymph nodes** smaller than 10 mm in long-axis diameter had significantly better overall and cancer-specific survival than patients with metastatic **lymph nodes** larger than 10 mm in diameter at histopathologic analysis following surgical resection.

Endoluminal ultrasound has improved accuracy in assessment of local **lymph** node metastases when compared with CT (80% compared with 51%) (41). However, patients suspected of having distant metastases are better assessed with CT of the thorax and abdomen (41).

Malignant Pleural Mesothelioma

Malignant pleural mesothelioma arises in the parietal and diaphragmatic pleura. The natural spread of mesothelioma is to the lungs through the visceral pleura and by local extension into the chest wall and diaphragm (42).

The anterior pleural **lymph**atics drain into the internal mammary **lymph nodes** in the upper and middle thorax (Fig 13) and the peridiaphragmatic **lymph nodes** in the lower thorax. The posterior pleural **lymph**atics drain into the extrapleural **lymph nodes**, which lie in the paraspinal extrapleural fat adjacent to the rib heads (Fig 14) (43).

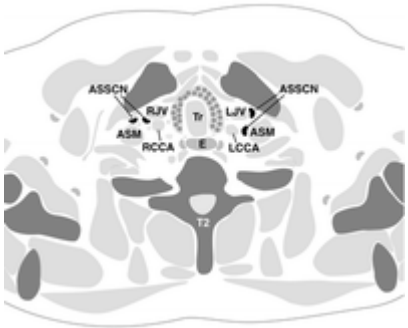

View larger version (39K):
[in this window]
[in a new window]
[Download PPT slide]

Figure 13a. Axial diagrams show the main regional drainage pathways (black **nodes**) for malignant mesothelioma. ***E*** = esophagus. **(a)** Diagram shows the anterior scalene/supraclavicular **nodes** *(ASSCN)*. *ASM* = anterior scalene muscle, *LCCA* = left common carotid artery, *LJV* = left internal jugular vein, *RCCA* = right common carotid artery, *RJV* = right internal jugular vein, *Tr* = trachea. **(b)** Diagram shows the extrapleural **nodes** *(EPN)*, internal mammary **nodes** *(IMN)*, lobar node *(LN)*, subcarinal node *(SCN)*, and segmental node *(SN)*. *AA* = ascending aorta, *Ao* = aorta, *LMB* = left main bronchus, *PA* = pulmonary artery, *RMB* = right main bronchus, *RPA* = right pulmonary artery, *SVC* = superior vena cava, *TD* = thoracic duct. **(c)** Diagram shows the pericardial fat **nodes** *(PCFN)*. *Ao* = aorta, *CS* = coronary sinus, *ECF* = epicardial fat, *LV* = left ventricle, *PCF* = pericardial fat, *RA* = right atrium, *RV* = right ventricle, *TD* = thoracic duct. **(d)** Diagram shows the anterior peridiaphragmatic **nodes** *(APDN)* and extrapleural **nodes** *(EPN)*. *Ao* = aorta.

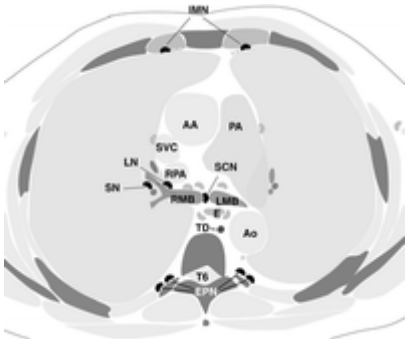

View larger version (39K):
[in this window]
[in a new window]
[Download PPT slide]

Figure 13b. Axial diagrams show the main regional drainage pathways (black **nodes**) for malignant mesothelioma. ***E*** = esophagus. **(a)** Diagram shows the anterior scalene/supraclavicular **nodes** *(ASSCN)*. *ASM* = anterior scalene muscle, *LCCA* = left common carotid artery, *LJV* = left internal jugular vein, *RCCA* = right common carotid artery, *RJV* = right internal jugular vein, *Tr* = trachea. **(b)** Diagram shows the extrapleural **nodes** *(EPN)*, internal mammary **nodes** *(IMN)*, lobar node *(LN)*, subcarinal node *(SCN)*, and segmental node *(SN)*. *AA* = ascending aorta, *Ao* = aorta, *LMB* = left main bronchus, *PA* = pulmonary artery, *RMB* = right main bronchus, *RPA* = right pulmonary artery, *SVC* = superior vena cava, *TD* = thoracic duct. **(c)** Diagram shows the pericardial fat **nodes** *(PCFN)*. *Ao* = aorta, *CS* = coronary sinus, *ECF* = epicardial fat, *LV* = left ventricle, *PCF* = pericardial fat, *RA* = right atrium, *RV* = right ventricle, *TD* = thoracic duct. **(d)** Diagram shows the anterior peridiaphragmatic **nodes** *(APDN)* and extrapleural **nodes** *(EPN)*. *Ao* = aorta.

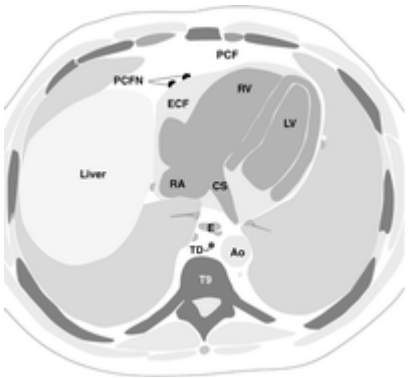

View larger version (42K):
[in this window]
[in a new window]
[Download PPT slide]

Figure 13c. Axial diagrams show the main regional drainage pathways (black **nodes**) for malignant mesothelioma. ***E*** = esophagus. **(a)** Diagram shows the anterior scalene/supraclavicular **nodes** *(ASSCN)*. *ASM* = anterior scalene muscle, *LCCA* = left common carotid artery, *LJV* = left internal jugular vein, *RCCA* = right common carotid artery, *RJV* = right internal jugular vein, *Tr* = trachea. **(b)** Diagram shows the extrapleural **nodes** *(EPN)*, internal mammary **nodes** *(IMN)*, lobar node *(LN)*, subcarinal node *(SCN)*, and segmental node *(SN)*. *AA* = ascending aorta, *Ao* = aorta, *LMB* = left main bronchus, *PA* = pulmonary artery, *RMB* = right main bronchus, *RPA* = right pulmonary artery, *SVC* = superior vena cava, *TD* = thoracic duct. **(c)** Diagram shows the pericardial fat **nodes** *(PCFN)*. *Ao* = aorta, *CS* = coronary sinus, *ECF* = epicardial fat, *LV* = left ventricle, *PCF* = pericardial fat, *RA* = right atrium, *RV* = right ventricle, *TD* = thoracic duct. **(d)** Diagram shows the anterior peridiaphragmatic **nodes** *(APDN)* and extrapleural **nodes** *(EPN)*. *Ao* = aorta.

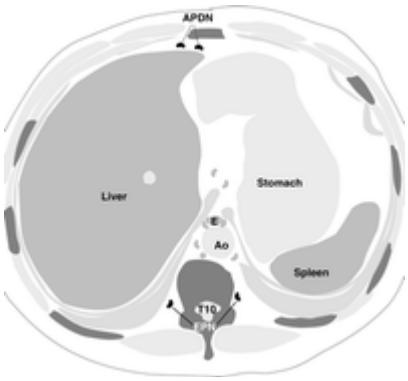

View larger version (38K):
[in this window]
[in a new window]
[Download PPT slide]

Figure 13d. Axial diagrams show the main regional drainage pathways (black **nodes**) for malignant mesothelioma. ***E*** = esophagus. **(a)** Diagram shows the anterior scalene/supraclavicular **nodes** *(ASSCN)*. *ASM* = anterior scalene muscle, *LCCA* = left common carotid artery, *LJV* = left internal jugular vein, *RCCA* = right common carotid artery, *RJV* = right internal jugular vein, *Tr* = trachea. **(b)** Diagram shows the extrapleural **nodes** *(EPN)*, internal mammary **nodes** *(IMN)*, lobar node *(LN)*, subcarinal node *(SCN)*, and segmental node *(SN)*. *AA* = ascending aorta, *Ao* = aorta, *LMB* = left main bronchus, *PA* = pulmonary artery, *RMB* = right main bronchus, *RPA* = right pulmonary artery, *SVC* = superior vena cava, *TD* = thoracic duct. **(c)** Diagram shows the pericardial fat **nodes** *(PCFN)*. *Ao* = aorta, *CS* = coronary sinus, *ECF* = epicardial fat, *LV* = left ventricle, *PCF* = pericardial fat, *RA* = right atrium, *RV* = right ventricle, *TD* = thoracic duct. **(d)** Diagram shows the anterior peridiaphragmatic **nodes** *(APDN)* and extrapleural **nodes** *(EPN)*. *Ao* = aorta.

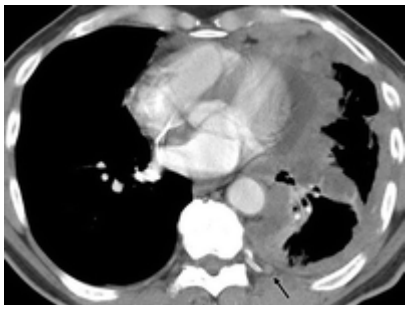

View larger version (104K):
[in this window]
[in a new window]
[Download PPT slide]

Figure 14a. Malignant mesothelioma in a 56-year-old man. **(a)** CT scan obtained at the level of the left atrium shows a 4-mm-diameter **lymph** node in the left extrapleural space (arrow). **(b)** CT scan obtained at the level of the clavicles shows a 2-cm-diameter left supraclavicular node (arrow), which was confirmed to be metastatic. This finding is defined as N3 disease. **(c)** CT scan obtained at the level of the interventricular septum shows a cluster of enhancing left peridiaphragmatic **nodes** (arrow). Note the irregular, enhancing, nodular pleural thickening and the loculated pleural effusion.

View larger version (119K):
[in this window]
[in a new window]
[Download PPT slide]

Figure 14b. Malignant mesothelioma in a 56-year-old man. **(a)** CT scan obtained at the level of the left atrium shows a 4-mm-diameter **lymph** node in the left extrapleural space (arrow). **(b)** CT scan obtained at the level of the clavicles shows a 2-cm-diameter left supraclavicular node (arrow), which was confirmed to be metastatic. This finding is defined as N3 disease. **(c)** CT scan obtained at the level of the interventricular septum shows a cluster of enhancing left peridiaphragmatic **nodes** (arrow). Note the irregular, enhancing, nodular pleural thickening and the loculated pleural effusion.

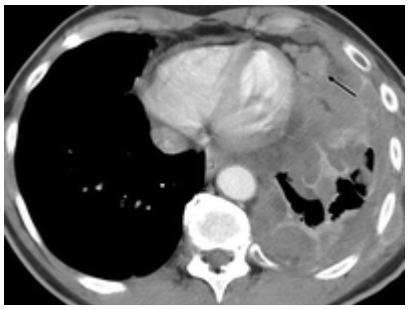

View larger version (104K):
[in this window]
[in a new window]
[Download PPT slide]

Figure 14c. Malignant mesothelioma in a 56-year-old man. **(a)** CT scan obtained at the level of the left atrium shows a 4-mm-diameter **lymph** node in the left extrapleural space (arrow). **(b)** CT scan obtained at the level of the clavicles shows a 2-cm-diameter left supraclavicular node (arrow), which was confirmed to be metastatic. This finding is defined as N3 disease. **(c)** CT scan obtained at the level of the interventricular septum shows a cluster of enhancing left peridiaphragmatic **nodes** (arrow). Note the irregular, enhancing, nodular pleural thickening and the loculated pleural effusion.

The diaphragm, which is commonly involved in mesothelioma, has a rich **lymph**atic network that communicates between the thorax and peritoneum. The anterior and lateral diaphragm **lymph**atics drain into the internal mammary and anterior peridiaphragmatic **lymph nodes**. The posterior diaphragm **lymph**atics drain into the paraaortic **lymph nodes** and **nodes** of the posterior mediastinum. Posterior **mediastinal lymph**atics drain superiorly and communicate with the middle mediastinum **lymph**atics. They may also drain inferiorly and involve the **lymph**atics of the gastrohepatic ligament and celiac axis (44).

A TNM staging system for malignant mesothelioma (Table 4) has been proposed by the International Mesothelioma Interest Group (45). N1 disease includes involvement of ipsilateral hilar or bronchopulmonary **nodes** (lobar, interlobar, and segmental **nodes**). N2 disease includes subcarinal and ipsilateral **mediastinal nodes**, including the internal mammary **nodes**. N3 disease includes contralateral **mediastinal** or internal mammary **nodes** and all supraclavicular **nodes** (Fig 14). The staging system is of limited value, as most patients present with advanced disease. However, there is a subset of patients who benefit from surgery and follow-up chemotherapy (46). These patients have epithelial histology and no evidence of extrapleural **nodes**, defined as **mediastinal** or peridiaphragmatic **nodes** (Fig 14a). Detection of these **lymph nodes** at CT would influence the care of this patient group.

View this table:
[in this window]
[in a new window]

TABLE 4. Nodal Staging in Malignant Mesothelioma according to the TNM Classification

Conclusions

There are different **lymph**atic drainage pathways within the thorax that are relevant in the staging of lung cancer, breast cancer, **lymph**oma, esophageal cancer, and malignant mesothelioma. It is important to carefully evaluate the specific nodal stations that drain the thoracic structures from which a primary tumor originates in order to properly search for metastatic spread. Owing to the limitations of size criteria in predicting nodal status, pathologic

confirmation is essential for true staging. CT is useful for guiding the surgeon or interventionalist to the most appropriate approach for nodal sampling. FDG PET, particularly when fused with CT, has a growing role in detecting the presence of disease in **lymph nodes** that appear normal at CT alone. However, the role of radiologic imaging extends beyond initial staging and interventional guidance and includes posttreatment assessment and the detection of recurrent disease. Therefore, it is essential, at all levels of cancer imaging, to identify the relevant **lymph** node regions and relate them to the primary tumor.

References

1. Beck E, Beattie EJ, Jr. The **lymph nodes** in the mediastinum. J Int Coll Surg 1958; 29:247-251.[Medline]

2. Genereux GP, Howie JL. Normal **mediastinal lymph** node size and number: CT and anatomic study. AJR Am J Roentgenol 1984; 142:1095-1100.[Abstract/Free Full Text]

3. Glazer GM, Gross BH, Quint LE, et al. Normal **mediastinal lymph nodes**: number and size according to American Thoracic Society mapping. AJR Am J Roentgenol 1985; 144:261-265.[Abstract/Free Full Text]

4. Schnyder PA, Gamsu G. CT of the pretracheal retrocaval space. AJR Am J Roentgenol 1981; 136:303-308.[Abstract/Free Full Text]

5. Toloza EM, Harpole L, McCrory DC. Noninvasive staging of non-small cell lung cancer: a review of the current evidence. Chest 2003; 123:137S-146S.

6. Graham NJ, Libshitz HI. Cascade of metastatic colorectal carcinoma from the liver to the anterior diaphragmatic **lymph nodes**. Acad Radiol 1995; 2:282-285.[CrossRef][Medline]

7. McLoud TC, Bourgouin PM, Greenberg RW, et al. Bronchogenic carcinoma: analysis of staging in the mediastinum with CT by correlative **lymph** node mapping and sampling. Radiology 1992; 182:319-323.[Abstract]

8. Pieterman RM, van Putten JWG, Meuzelaar JJ, et al. Preoperative staging of non-small cell lung cancer with positron emission tomography. N Engl J Med 2000; 343:254-261.[Abstract/Free Full Text]

9. Valk PE, Pounds TR, Hopkins DM, et al. Staging non-small cell lung cancer by whole-body positron emission tomographic imaging. Ann Thorac Surg 1995; 60:1573-1582.[Abstract/Free Full Text]

10. Mountain CF, Dresler CM. Regional **lymph** node classification for lung cancer staging. Chest 1997; 111:1718-1723.[Abstract/Free Full Text]

11. Fraser RS, Muller NL, Colman N, Pare PD. Fraser and Pare's diagnosis of diseases of the chest 4th ed. Philadelphia, Pa: Saunders, 1999; 172-195.

12. Takizawa T, Terashima M, Koike T, Akamatsu H, Kurita Y, Yokoyama A. **Mediastinal lymph** node metastasis in patients with clinical stage 1 peripheral non-small cell lung cancer. J Thorac Cardiovasc Surg 1997; 113:248-252.[Abstract/Free Full Text]

13. Ota S, Inaba H, Yoshida H. Rational **lymph** node dissection for lung cancer according to the occurrence lobe and histological type. Kyobu Geka 2001; 54:1073-1078.[Medline]

14. Riquet M, Hidden G, Debesse B. Direct **lymph**atic drainage of lung segments to the **mediastinal nodes**: an anatomic study on 260 adults. J Thorac Cardiovasc Surg 1989; 97:623-632.[Abstract]

15. Riquet M, Barthes FL, Souilamas R, et al. Thoracic duct tributaries from intrathoracic organs. Ann Thorac Surg 2002; 73:892-899.[Abstract/Free Full Text]

16. Greene FL, Page DL, Fleming ID, et al. eds. AJCC cancer staging manual 6th ed. New York, NY: Springer-Verlag, 2002; 91-241.

17. Asamura H, Suzuki K, Kondo H, Tsuchiya R. Where is the boundary between N1 and N2 stations in lung cancer? Ann Thorac Surg 2000; 70:1839-1846.[Abstract/Free Full Text]

18. Crisci R, Di Cesare E, Lupattelli L, et al. MR study of N2 disease in lung cancer: contrast-enhanced method using gadolinium-DTPA. Eur J Cardiothorac Surg 1997; 11:214-217.[Abstract]

19. Rouviere H. Anatomy of the human **lymph**atic system Tobias MJ, trans. Ann Arbor, Mich: Edwards, 1938.

20. Tanis PJ, Nieweg OE, Olmos RA, et al. Anatomy and physiology of **lymph**atic drainage of the breast from the perspective of sentinel node biopsy. J Am Coll Surg 2001; 192:399-409.[CrossRef][Medline]

21. Borgstein PJ, Meijer S, Pijpers RJ, et al. Functional **lymph**atic anatomy for sentinel node biopsy in breast cancer: echoes from the past and the periareolar blue method. Ann Surg 2000; 232:81-89.[CrossRef][Medline]

22. Wallace S, Jing BS. Carcinoma. In: Clouse ME, eds. Clinical **lymph**ography: Golden's diagnostic radiology. Baltimore, Md: Williams & Wilkins, 1977; 185-273.

23. Sappey PC. Traite d'anatomie descriptive 4th ed. Paris, France: A. Delahaye et E. Lecrosnier, 1888.

24. Krag D. Minimal invasive staging for breast cancer: clinical experience with sentinel **lymph** node biopsy. Semin Oncol 2001; 28:229-235.[CrossRef][Medline]

25. Mansel RE, Khonji NI, Clarke D. History, present status and future of sentinel node biopsy in breast cancer. Acta Oncol 2000; 39:265-268.[CrossRef][Medline]

26. Whitworth P, McMasters MK, Tafra L, Edwards M. State-of-the-art **lymph** node staging for breast cancer in the year 2000. Am J Surg 2000; 180:262-267.[CrossRef][Medline]

27. Miyauchi M, Yamamoto N, I Manaka N, Matsumoto M. Computed tomography for preoperative evaluation of axillary nodal status in breast cancer. Breast Cancer 1999; 6:243-248.[Medline]

28. March DE, Wechsler RJ, Kurtz AB, et al. CT-pathologic correlation of axillary **lymph nodes** in breast carcinoma. J Comput Assist Tomogr 1991; 15:440-444.[Medline]

29. Hata Y, Ogawa Y, Nishioka A, et al. Thin section computed tomography in the prone position for detection of axillary **lymph** node metastases in breast cancer. Oncol Rep 1998; 5:1403-1406.[Medline]

30. Yuen S, Sawai K, Ushijima Y, et al. Evaluation of axillary status in breast cancer: CT-based determination of sentinel **lymph** node size. Acta Radiol 2002; 43:579-586.[CrossRef][Medline]

31. Harris NL, Jaffe ES, Stein H, et al. A revised European-American classification of **lymph**oid neoplasms: a proposal from the International **Lymph**oma Study Group. Blood 1994; 84:1361-1392.[Free Full Text]

32. Castellino RA, Blank N, Hoppe RT, Cho C. Hodgkin disease: contributions of chest CT in the initial staging evaluation. Radiology 1986; 160:603-605.[Abstract]

33. Castellino RA, Hilton S, O'Brien JP, Portlock CS. Non-Hodgkin **lymph**oma: contribution of chest CT in the initial staging evaluation. Radiology 1996; 199:129-132.[Abstract/Free Full Text]

34. Aquino SL, Chen MY, Kuo WT, Chiles C. The CT appearance of pleural and extrapleural disease in **lymph**oma. Clin Radiol 1999; 54:647-650.[CrossRef][Medline]

35. Apter S, Avigdor A, Gayer G, Portnoy O, Zissin R, Hertz M. Calcification in **lymph**oma occurring before therapy: CT features and clinical correlation. AJR Am J Roentgenol 2002; 178:935-938.[Abstract/Free Full Text]

36. Patti MG, Gantert W, Way WL. Surgery of the esophagus: anatomy and physiology. Surg Clin North Am 1997; 77:959-970.[CrossRef][Medline]

37. Riquet M, Saab M, Le Pimpec Barthes F, Hidden G. **Lymph**atic drainage of the esophagus in the adult. Surg Radiol Anat 1993; 15:209-211.[CrossRef][Medline]

38. Akiyama H, Tsurumaru M, Kawamura T, et al. Principles of surgical treatment for carcinoma of the esophagus: analysis of **lymph** node involvement. Ann Surg 1981; 194:438-446.[Medline]

39. Schroder W, Baldus SE, Monig SP, et al. **Lymph** node staging of esophageal squamous cell carcinoma in patients with and without neoadjuvant radiochemotherapy: histomorphologic analysis. World J Surg 2002; 26:584-587.[CrossRef][Medline]

40. Dhar DK, Tachibana M, Kinukawa N, et al. The prognostic significance of **lymph** node size in patients with squamous esophageal cancer. Ann Surg Oncol 2002; 9:1010-1016.[Abstract/Free Full Text]

41. Tio TL, Coene PP, Udding J, et al. Endosonography and computed tomography of esophageal carcinoma: preoperative classification compared to the new (1987) TNM system. Gastroenterology 1989; 96:1478-1486.[Medline]

42. Antman KH, Pass HI, Schiff PB. Malignant mesothelioma. In: DeVita VT, Hellman S, Rosenberg SA, eds. Cancer: principles and practice of oncology. New York, NY: Lippincott Williams & Wilkins, 2001; 1943-1969.

43. Light RW. Pleural diseases 4th ed. Philadelphia, Pa: Lippincott Williams & Wilkins, 2001; 1-7.

44. Souilamas R, Hidden G, Riquet M. **Mediastinal lymph**atic efferents from the diaphragm. Surg Radiol Anat 2001; 23:159-162.[CrossRef][Medline]

45. Rusch VW. A proposed new international TNM staging system for malignant pleural mesothelioma: from the International Mesothelioma Interest Group. Chest 1995; 108:1122-1128.[Abstract/Free Full Text]

46. Sugarbaker DJ, Flores RM, Jaklitsch MT, et al. Resection margins, extrapleural nodal status and cell type determine postoperative long-term survival in trimodality therapy of malignant pleural mesothelioma: results in 183 patients. J Thorac Cardiovasc Surg 1999; 117:54-65.[Abstract/Free Full Text]